J. Fluid Mech. (1966), *vol.* 25, *part* 3, *pp.* 495–512
Printed in Great Britain

Exploratory measurements in spiral turbulence

By CHARLES VAN ATTA†
University of California, San Diego,
Department of the Aerospace and Mechanical Engineering Sciences,
La Jolla, California

(Received 2 August 1965)

The present experiments lay a foundation for a detailed study of interface propagation in a mixed laminar–turbulent flow between counter-rotating concentric cylinders. Such mixed flows, including one particularly well-organized pattern called spiral turbulence, are found to be a dominant feature of transition in Couette flow. In spiral turbulence, the laminar and turbulent regions of the flow form an alternating pattern of helical stripes, rotating with approximately the mean angular velocity of the two cylinders. Stable right-handed or left-handed spirals occur with equal probability when the flow is established from rest. Hot-wire measurements have been made of the mean cross-sectional shape of the interfaces in the axial mid-plane for a spiral-turbulent flow having low dispersion in the interface position. A nose of turbulence associated with the leading interface projects into the laminar region near the outer cylinder, while a corresponding tail is associated with the trailing interface near the inner cylinder. Fluctuations in interface position and in apparent length of the turbulent region are closely Gaussian, and the fluctuations are rapid compared with the period of rotation of either cylinder.

1. Introduction

Under certain conditions, a pattern of alternating helical stripes of laminar and turbulent flow can be observed in the gap between concentric rotating cylinders. This phenomenon, now called spiral turbulence, was first observed by Oguro (unpublished) and Coles (1962) in a large rotating-cylinder apparatus at GALCIT.‡ Oguro's measurements were made with the inner cylinder at rest and the outer cylinder rotating at high speed. A stable mixed laminar–turbulent configuration was found, with the laminar flow confined to narrow regions near both walls. The pattern rotated with approximately half the angular velocity of the outer cylinder. At about this same time, Coles obtained the photograph shown in figure 1 (plate 1), using a smaller apparatus and a suspension of aluminium particles in silicone oil as a means of flow visualization. The mottled areas in the photograph indicate turbulent flow, and the smoother areas indicate laminar flow. In this case, the cylinders were rotating in opposite directions at relatively

† Formerly at the Jet Propulsion Laboratory, California Institute of Technology, Pasadena, California.

‡ Graduate Aeronautical Laboratories, California Institute of Technology.

low speed. The helical pattern, whether right- or left-handed, rotated at approximately the mean angular velocity of the two cylinders without changing its general shape.

Oguro concluded that fluid elements move on the average in nearly circular paths, so that an element near either wall repeatedly traverses the pattern, participating alternately in the laminar and turbulent motion. Whether or not this conclusion is correct, it is certain that the volume of turbulent fluid in spiral turbulence is statistically constant. Hence any flow into the turbulent region must be balanced by an equal flow out. Barring the unlikely event that there is no net flow in either direction, it follows that interfaces separating regions of laminar and turbulent flow must be of two kinds. One kind, involving transition in the usual sense, propagates into the laminar region; the other kind, involving inverse or anti-transition, propagates into the *turbulent* region.

Given this property of spiral turbulence, what is the mechanism by which turbulence disappears at an anti-transition interface? The qualitative similarity in flow behaviour at the leading and trailing interfaces, as illustrated by a typical hot-wire signal in figure 2 (plate 2), suggests that this mechanism may not be entirely viscous or diffusive in nature. The long-range object of the present research is to study this question by measuring the local rate of energy transfer between mean flow and turbulence, especially near the interfaces. The experimental technique is both new and difficult, requiring thousands of accurate measurements of the instantaneous velocity vector at each of hundreds of known points in the flow pattern. Although the research is well advanced (some progress has been summarized by Van Atta 1964), it is not yet complete, and the dominant energy processes in the flow are still unknown. The present paper will therefore deal only with some preliminary and peripheral results, obtained for the most part by analogue, rather than digital, techniques. In particular, it was obvious from the beginning that only one spiral flow could reasonably be studied in the necessary detail. Exploratory measurements were therefore carried out in 1961 and 1962 to find a suitable flow and to determine some of its simpler properties. These exploratory measurements are the subject of the present paper.

The symbols used throughout the paper are as follows:

f_i Frequency of interface pattern as observed from inner cylinder.
f_o Frequency of interface pattern as observed from outer cylinder.
l_t Apparent length of turbulent region at $r = \text{const.}$
L Length of annular working space = distance between end plates.
P Time interval between probe crossings of a given interface; $\langle P \rangle \propto 1/f$.
δ $P - \langle P \rangle$.
r Radial co-ordinate.
r_i Radius of inner cylinder.
r_o Radius of outer cylinder.
R_i Reynolds number of inner cylinder; $R_i = \omega_i r_i^2/\nu$.
R_o Reynolds number of outer cylinder; $R_o = \omega_o r_o^2/\nu$.
z Axial co-ordinate measured from mid-plane of symmetry.
α Pitch angle of helix measured with respect to plane $z = \text{const.}$
γ Intermittency factor.

θ Fluctuating component of interface position.
Θ Angular co-ordinate.
σ Standard deviation of random variable.
ν Kinematic viscosity of air.
ω_i Angular velocity of inner cylinder.
ω_o Angular velocity of outer cylinder.
ω_t Mean angular velocity of spiral turbulence in laboratory co-ordinates.
$\langle\rangle$ Stochastic mean value.

2. Apparatus

The experiments were performed in the large rotating-cylinder apparatus described by Coles (1965). The working fluid was air. The nominal inner and outer diameters of the annular working space were 32 and 36 in., respectively. The axial length of the working space could be varied in the range from 34 to 55 in. by means of adjustable end plates, which prevented outside disturbances from propagating into the annulus. The end plates rotated with the outer cylinder, and there was a discontinuity in velocity [of magnitude $(\omega_o - \omega_i) r_i$] where the end plates met the inner cylinder. Each cylinder was equipped with a slip-ring assembly to allow hot-wire and other signals to commute between laboratory and rotating frames. For the exploratory measurements described here, the hot-wire instrumentation usually consisted of single-wire probes operated at constant current. The stem of each probe was a length of 0·042 in. OD stainless-steel tubing with a 90° bend. The tubing served as one electrical conductor. An insulated central conductor of 0·013 in. diameter drill rod protruded from both ends of the tubing. The hot wire (0·0001 in. diameter) was soldered between the sharpened tip of this central conductor and the sharpened tip of another short length of drill rod soldered to the tube wall. The probes were mounted on aluminium pads, fitting snugly into 0·625 in. diameter holes in the wall of each cylinder and conforming to the curvature of the cylinder on the face exposed to the flow.

The intermittency meter, which was designed and constructed by Oguro, had a cathode-ray tube and photomultiplier tube as basic elements. The lowest frequencies in the hot-wire signal, corresponding to mean-flow variations, were filtered out, and the amplitude of the resulting signal was adjusted until the oscilloscope trace was completely masked (during any laminar intervals) by a thin horizontal strip of opaque tape. Turbulent signals were detected by a photomultiplier tube, looking at the oscilloscope face through a lens system. The output of the photomultiplier tube, smoothed by a suitable choice of phosphor for the cathode-ray tube and also by a low-pass filter, was converted to a square wave and used to gate an oscillator signal into a counter during intervals of turbulent flow. To obtain the intermittency factor, the reading of the gated counter was divided by the reading of a second free-running counter driven by the same time base. A half-silvered mirror allowed observation of the partially masked signal without disturbing the discrimination process. The intermittency meter was calibrated by the usual subjective method; i.e. by adjusting the time constants and trigger levels until the gate signals appeared to coincide with the beginning and end of turbulence in the untreated signal.

Operating conditions for the cylinders were defined by Reynolds numbers based on radius and surface velocity. The angular velocity of the outer cylinder, which always rotated in the same direction, was arbitrarily taken as negative. The Reynolds numbers for the outer and inner cylinders, R_o and R_i, took the signs of ω_o and ω_i, respectively. For most of the experiments, the cylinders turned in opposite directions, and ω_i and R_i were positive.

3. Observations of transition

In the earliest experiments, the angular velocities of the two cylinders were unsystematically increased until transition to fully or partially turbulent flow occurred. Except where noted, the length of the working space was kept fixed at its maximum value of 54·7 in. The flow was normally observed at mid-radius ($r = 17$ in.) in the axial mid-plane of the cylinders ($z = 0$), using hot-wire probes mounted on either cylinder. As expected, intermittency was found to be the dominant feature of transition when the cylinders turned in opposite directions. For a wide range of Reynolds numbers, the hot-wire signals showed a regular alternation between laminar and turbulent flow, as in figure 2, or else showed turbulent flow in which the amplitude of the turbulence varied periodically with comparable frequency. More irregular flows were also observed, in which the laminar and turbulent regions were not as uniformly compartmented. In some instances, a tendency was noted for successive turbulent regions to combine, swallowing up the laminar region. In other cases, turbulence sometimes appeared briefly in the normally laminar portion of the signal. The latter behaviour is believed to be due to large irregularities in the interface or to rapid fluctuations in interface position, rather than to islands of turbulence separated from the main body of turbulent fluid.

To investigate more closely the manner in which these intermittently turbulent flows were established, the speeds of the cylinders were varied more systematically. With laminar flow in the annulus, and with the Reynolds number R_o of the outer cylinder held constant, the angular velocity of the inner cylinder was increased slowly from zero in the opposite direction. Provided that $-R_o$ was neither too large nor too small, the flow remained entirely laminar up to a repeatable critical value R_{ic}, at which turbulence appeared with catastrophic suddenness. In some cases, the subsequent signal showed a periodic alternation between laminar and turbulent flow; and in other cases it was fully turbulent, with or without an observable low-frequency variation in amplitude. By making several runs at fixed R_o, with R_i increasing as slowly as possible, a lower bound was established for R_{ic}, as shown in figure 3.

For $-R_o$ less than about 100,000, this experimental boundary for catastrophic transition follows the trend of the theoretical Taylor instability boundary. In this range, transition is probably caused by breakdown of the toroidal vortices which are known to exist above the Taylor boundary, and to increase in strength as R_i increases. The Taylor instability itself, since it produces no circumferential flow variation, could not be detected experimentally.

For $-R_o$ greater than about 100,000, a different behaviour was found; R_{ic} decreased to zero as $-R_o$ increased. The stability analysis of Schultz-Grunow

(1959) indicates that flow below the Taylor boundary is also stable to infinitesimal disturbances of Tollmien–Schlichting type. At higher Reynolds numbers, however, transition may be initiated by either of two *finite* disturbances that always exist in the flow. These are (*a*) the vorticity concentration at the end plate, and (*b*) the probe wake. A very similar transition boundary was observed by Coles (1965, figure 2), employing a flow-visualization technique which avoided

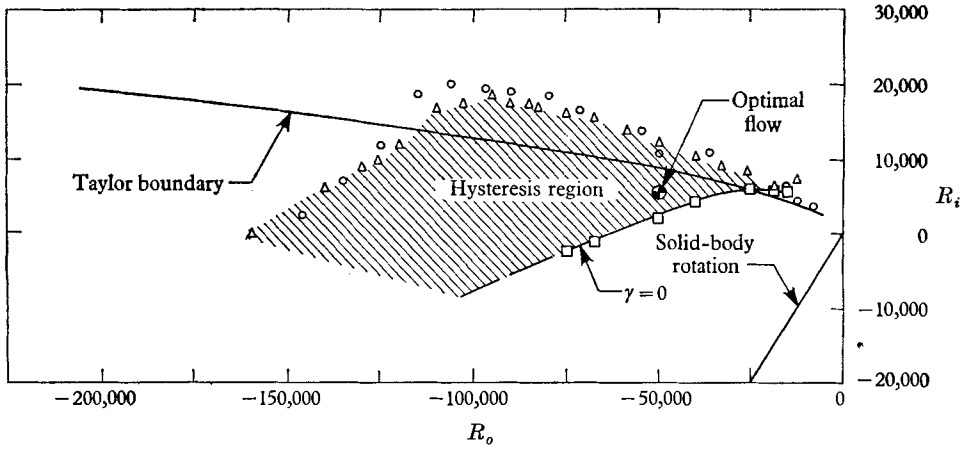

FIGURE 3. Boundary for catastrophic transition. Circles and triangles show position of transition boundary (approached from below). Squares show boundary for permanent disappearance of turbulence (approached from above). △□, l = 54·7 in.; ○, l = 34·7 in.

probe disturbances. From his visual observations, he concluded that transition began in the vorticity concentrations at the end plates, which were split at mid-radius. In the present experiments, the vorticity concentrations were modified by rotating the end plates with the outer cylinder. The Reynolds number $-R_o$ at which the influence of the end plates is first seen increased from about 40,000 (Coles's data) to about 100,000. As may be seen in figure 3, there is also a small systematic shift in the transition boundary when the length of the working space is decreased by 40 %. The latter result is consistent with a study by Coles & Van Atta (1966) showing that the laminar velocity profile at large Reynolds numbers can be profoundly influenced even by relatively distant end plates.

The effect of probe disturbances was not investigated in detail. At three speeds, runs with different radial probe positions showed no significant change in the transition Reynolds number R_{ic}, suggesting that the probe played no important role in initiating the turbulence. On the other hand, it was found during probe calibrations with the inner cylinder at rest (Coles & Van Atta 1966, figure 3) that the wake of a larger multiple hot-wire probe definitely triggered transition when the probe Reynolds number (based on stem diameter and relative velocity at the tip) exceeded a value of about 300.

When R_i was increased beyond R_{ic}, the flow became increasingly turbulent (γ increasing). In all cases, a value of R_i could be reached for which the intermittency factor at mid-gap was unity, and the turbulence was of uniform intensity. When R_i was first increased to R_{ic} and then decreased, turbulence persisted, the

alternations between laminar and turbulent flow usually becoming at first more regular and sharply defined. As R_i was further decreased, both the intervals between bursts of turbulence and the lengths of the bursts became increasingly random, until the turbulence degenerated and disappeared at a lower critical Reynolds number. This lower bound, denoted by the curve $\gamma = 0$ in figure 3, was established by varying the speed of the inner cylinder as slowly as possible. For sufficiently large $-R_o$, intermittency persisted even when both cylinders rotated in the same sense.

The hysteresis just described means that two distinct states (one completely laminar, the other partially or fully turbulent) could be observed for certain values of R_o and R_i. The intermittent turbulent flows throughout the transition region, as characterized either by the intermittency factor or by the angular velocity of the interfaces (see § 4), seemed to be unique, no matter how the cylinder speeds approached their final steady values. For example, if the angular velocity of the inner cylinder was fixed and the angular velocity of the outer cylinder was increased slowly from rest, transition could occur gradually through a progression of increasingly irregular motions,† but the final state of the flow was the same unique function of the two Reynolds numbers.

4. Interface propagation velocity

In the region of spiral turbulence, the average angular velocity of the interfaces relative to the laboratory, ω_t, and the number of turbulent regions propagating around the annulus, N, were calculated from the frequency of the pattern as observed from probes on both cylinders. Frequencies were obtained by timing 30 or more cycles of the flow pattern with a stopwatch. The relevant equations, in which f_o and f_i are the frequencies observed from the outer and inner cylinders, respectively, are $\omega_t = (\omega_i f_o + \omega_o f_i)/(f_o + f_i)$ and $N = 2\pi(f_o + f_i)/(\omega_i - \omega_o)$. In all cases, the number of turbulent regions calculated was unity (to one part in a thousand). The interfaces always travelled in the same direction as the outer cylinder, which was always rotating faster than the inner cylinder.

As shown in figure 4, the quantity $2\omega_t/(\omega_o + \omega_i)$, although a weak function of Reynolds number over most of the transition region, is nearly equal to unity for most of the observations. In other words, ω_t is approximately equal to the mean angular velocity of the two cylinders; the turbulence moves as if it were being convected with the mean angular velocity of the fluid. Above the Taylor boundary, there is a relatively rapid rate of increase in $2\omega_t/(\omega_o + \omega_i)$ in figure 4, so that instability of the Taylor type may play a role even after turbulence has become established.

For $-R_o$ less than 100,000, most of the data in figure 4 were obtained with hot wires located at mid-gap; but, for larger values of $-R_o$, the signals at mid-gap lost their modulated character as the intensity of the turbulence became independent of Θ. Since the flow near the outer cylinder remained periodically intermittent for larger Reynolds numbers, most of the ω_t data for $-R_o > 100{,}000$ were obtained at $r = 17{\cdot}9$ in.

† Because of the shape of the transition boundary in figure 3, catastrophic transition will not be observed when operating in this manner unless R_i is less than about 20,000.

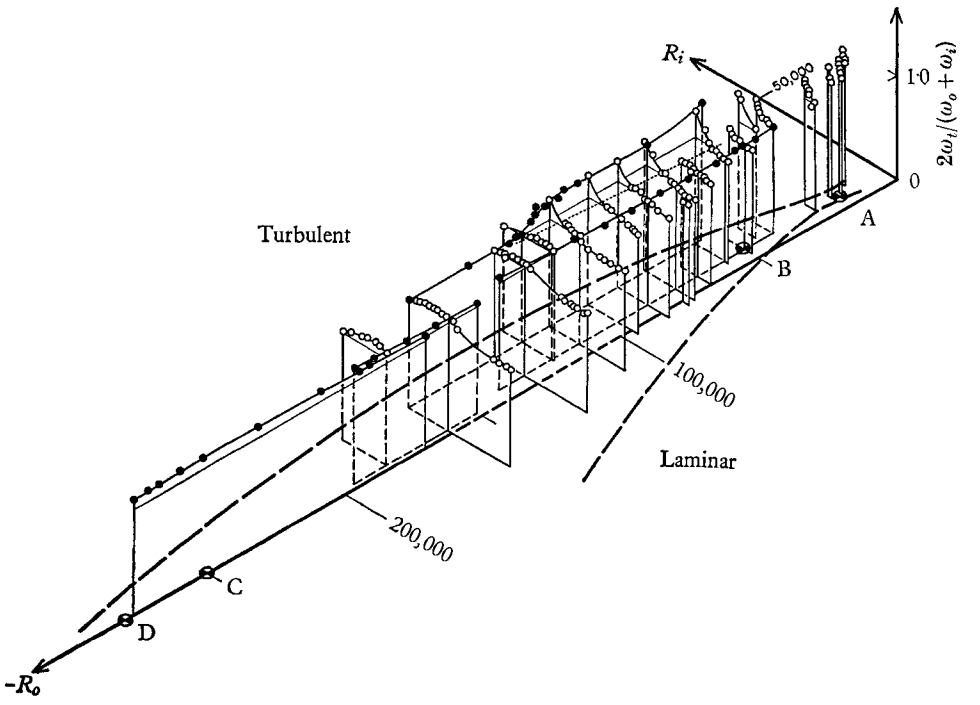

FIGURE 4. Angular velocity ω_t of spiral turbulence pattern. ○, Data for constant R_o; ●, data for constant R_i; ------, Taylor boundary. Point A corresponds to the photograph in figure 1 (plate 1); point B to optimal flow; points C and D to flows studied by Oguro (unpublished).

5. Evidence for helical structure

To determine whether the flow in the large machine had a spiral pattern, as in figure 1 (plate 1), the differences in arrival times of a given interface at three probes having different axial locations were roughly measured for a few cases with R_o between $-18{,}000$ and $-60{,}000$. The time intervals were measured from photographic records obtained with a dual-beam oscilloscope or (at the lower speeds) with a stopwatch. The probes were all mounted on the outer cylinder, at $r = 17$ in. One probe was at $z = 0$, $\Theta = 0°$, while the other two probes were located at $z = -24$ in., $\Theta = 0°$ and $z = -12$ in., $\Theta = +15°$. The hypothetical helix angle was computed from the average time interval between the beginning of successive turbulent bursts in the signals from each pair of probes.

Since the hand of the helix was not known *a priori*, the mean helix angle was computed twice, assuming first a left-handed and then a right-handed helix. The angles calculated from different pairs either differed substantially (usually by about 20°, or roughly a factor of two) or else were very close together (within 1 or 2° in several cases). For two cases in which the calculated angles differed by less than 1°, the calculated helix angles were 27·5° and 28·0°, measured with respect to a plane $z = \text{const}$. The latter value was for $R_o = -18{,}300$, $R_i = 6{,}370$, fairly close to the operating point of the smaller machine in figure 1 ($R_o = -15{,}880$, $R_i = 5250$). One full turn of a helix with a pitch angle α of 28° [$\tan\alpha = (dz/r\,d\Theta)$]

would have an axial length of 57 in., implying that the helix in the large machine was also wrapped nearly once around the annulus, whose actual length was 54·7 in.

It was also found that both right- and left-handed helical patterns had been observed. In one case, measurements taken several minutes apart showed that the helix had changed hand while both cylinder speeds remained constant. This transition from one hand to the other was observed as a brief period (about 15 sec, or 5 normal cycles of the flow) of very irregular, fully turbulent flow. These measurements were relatively crude, since only about 10 cycles of the flow were used to obtain the average helix angles, but they did confirm both the helical structure of the flow and the existence of right- and left-handed configurations in the large apparatus.

Further evidence for right- and left-handed helices was obtained during a preliminary study of the axial flow component for the optimal spiral-turbulence configuration discussed in § 6 below. The difference signal from two hot wires forming a V-array in the surface $r = 16{\cdot}5$ in. showed a strongly periodic low-frequency component, with extreme values in the laminar and turbulent portions of the cycle (cf. figure 2, plate 2). The sensitivity of the wire array to changes in flow angle was measured by yawing the probe in a laminar flow, and the over-all flow deflexion per cycle in the spiral turbulence was estimated to be about 10°. When the intermittent flow was repeatedly established from rest, it was found that the low-frequency part of the difference signal was sometimes reflected in the horizontal axis, showing the random occurrence of two flows having opposite hands. The two hands deflected the mean flow in opposite directions as corresponding laminar and turbulent regions of the flow pattern were traversed.

6. An optimal flow

A principal objective of the general transition survey was to find the most regular mixed-flow configuration obtainable with the apparatus, using two criteria: (1) sharply delineated laminar and turbulent regions for all radial locations in the annulus, and (2) low dispersion for fluctuations of the interface geometry about its mean position in suitable rotating co-ordinates. A group of extremely stable mixed flows satisfying these criteria was noted in the region $R_o = -40{,}000$ to $-50{,}000$, $R_i = 3500$ to 10,000. Visual inspection of hot-wire signals in this region indicated that the most regular flow, and thus the most suitable flow for the elaborate measurements mentioned in § 1, would be found in the neighbourhood of $R_o = -50{,}000$, with R_i between 5000 and 6000.

With R_o fixed at $-48{,}000$, a quantitative measure of the regularity of the flow at various values of R_i was next obtained by measuring the dispersion in the time interval P between successive observations of the same interface at $r = 17$ in. The intermittency meter produced a square wave whose positive-going edges marked the beginning of turbulence for each cycle. For several values of R_i, 300 time intervals between successive edges were measured with an electronic counter and recorded manually. The result in each case was a nearly Gaussian distribution function for P; a typical example is shown in figure 5. (For a normally

distributed variable, the scales are arranged to produce a straight line with a slope inversely proportional to the standard deviation.) Given the mean period $\langle P \rangle$ and the standard deviation σ, the ratio $\sigma/\langle P \rangle$ provides a direct measure of relative dispersion in interface position at different Reynolds numbers, as shown in figure 6. The brackets in the figure are an estimate of the uncertainty in σ arising from graphical determination of the slope in figure 5. The plot of

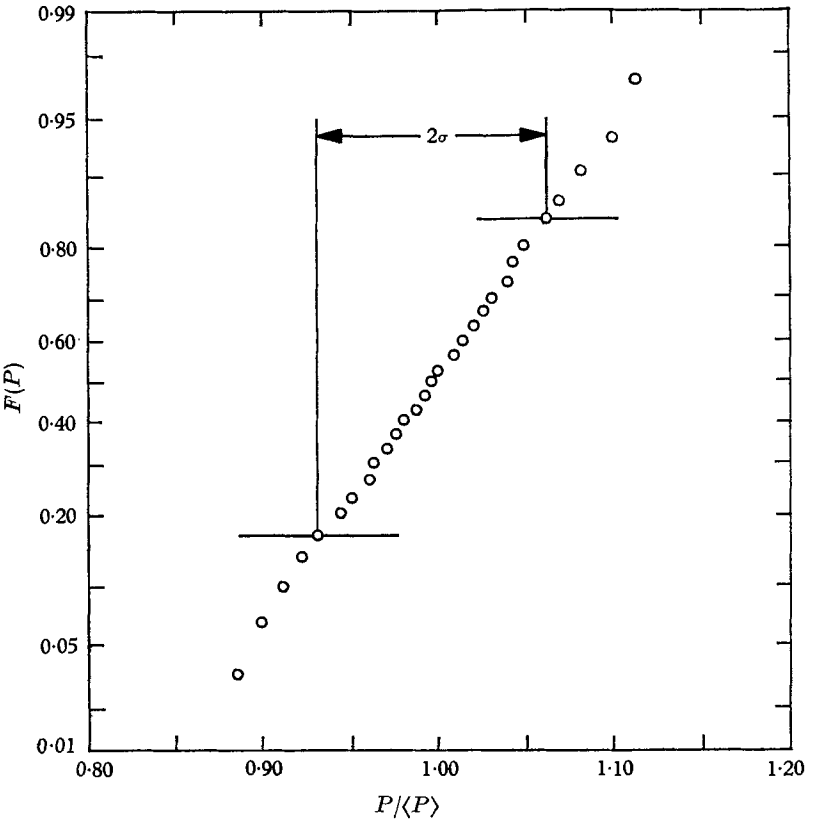

FIGURE 5. Typical distribution function for interface position at $r = 17$ in. $R_o = -48{,}000$; $R_i = 4225$.

$\sigma/\langle P \rangle$ *vs.* R_i determines an optimal flow, since there is a minimum near $R_i = 5600$. The operating point $R_o = -50{,}000$, $R_i = 5600$ was therefore chosen for further exploratory measurements. In the neighbourhood of this operating point, according to figure 4, the normalized angular velocity of the turbulence is practically independent of both R_o and R_i. The operating point for the optimal flow lies in the hysteresis region† in figures 3 and 6, approximately half-way between the Taylor boundary and the boundary $\gamma = 0$ below which turbulence cannot persist.

† It follows that it is possible, although perhaps not convenient or desirable, to establish a laminar flow for probe calibration at precisely the same operating conditions as for the optimal spiral turbulent flow.

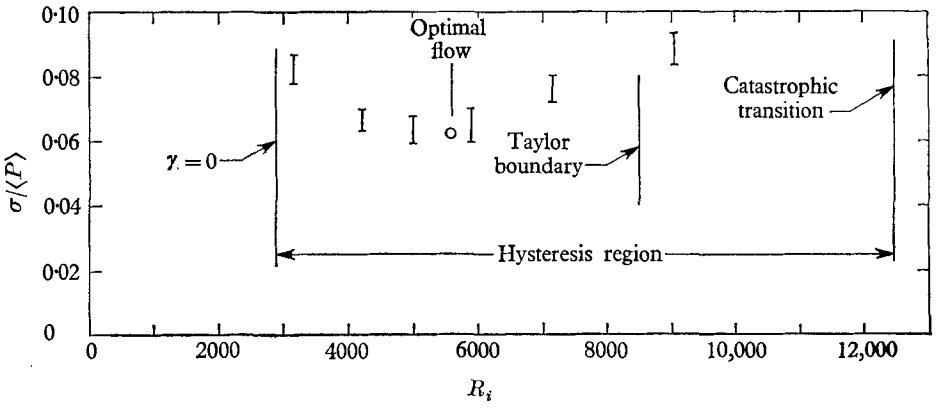

FIGURE 6. Standard deviation of interface position at $r = 17$ in. as function of R_i for fixed $R_o = -48{,}000$. Data based on 300 cycles of flow for each value of R_i. Data are for trailing interface (see figures 11 and 12).

7. Intermittency measurements in the optimal flow

All measurements of γ reported here were obtained by averaging over at least 100 cycles of the pattern (approximately 5 min.). The pass band of the γ-meter filter (Kronhite 300-M) was 4 cycles/sec to 20,000 cycles/sec, but there was very little turbulent energy above 200 cycles/sec. For $R_o = -50{,}000$, the variation of γ with R_i, measured at $z = 0$ for three different radii, is plotted in figure 7. With increasing Reynolds number, γ increased more slowly near the walls than in the centre of the gap, increasing most slowly near the outer cylinder. Thus the flow can be essentially fully turbulent near the inner cylinder and at mid-gap, while the intermittency factor near the outer cylinder is still as low as 0·7. With regard to the radial distribution of γ, the flow studied by Oguro ($R_o = -250{,}000$, $R_i = 0$) was of this type.

In figure 7, the radial distribution of γ at $z = 0$ for $R_o = -50{,}000$, $R_i = 5600$ (the optimal flow) shows a broad maximum at mid-gap, around which the distribution is nearly symmetrical. The dispersion in the time interval P between successive observations of the same interface, and the dispersion in the apparent length of the turbulent region l_t, are generally larger near the walls than in the centre of the gap. For three radii, the dispersion in l_t was found by measuring individual intervals during which the intermittency meter indicated turbulent flow. This was accomplished by manually resetting a gated counter to zero during an interval of laminar flow and recording the number displayed on the counter after an interval of turbulent flow. From the approximately Gaussian distribution functions shown in figure 8, the normalized dispersion in l_t at points 0·1 in. from each wall was estimated to be perhaps 50–100 % larger than at mid-gap. The intervals between observations of the same interface showed a corresponding increase in dispersion near the walls, being nearly 60 % larger at $r = 16{\cdot}25$ in. than in the centre of the gap (figure 9).

For all of these measurements, the intermittency factor γ is defined as the fraction of time during which turbulent flow is observed using a *single moving*

probe at fixed radius. Measured correlations of time intervals between successive crossings of the same interface (see figure 13 and Appendix), indicate that fluctuations in interface position have a characteristic time considerably less than the time required by the probe to traverse once through the flow pattern. Con-

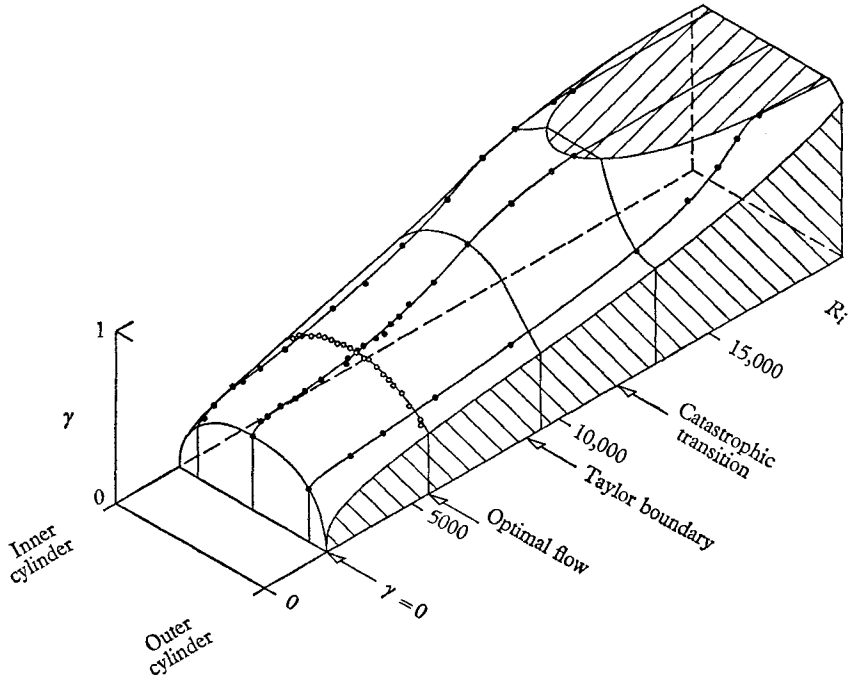

FIGURE 7. ●, Variation of γ with R_i for fixed R_o and fixed radius; ○, radial distribution of γ for $R_i = 5600$, $R_o = -50{,}000$.

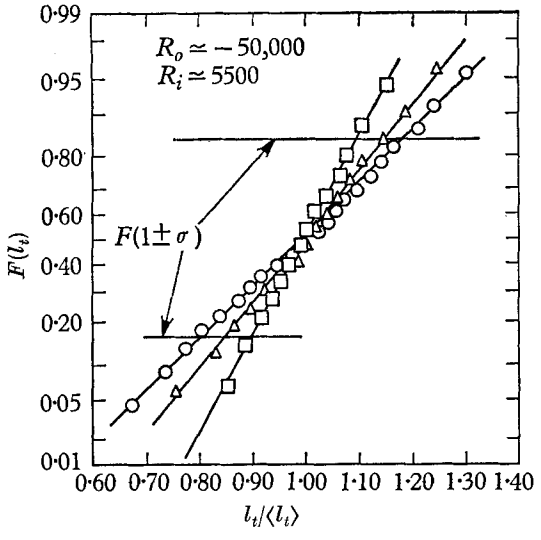

FIGURE 8. Distribution of apparent length of turbulent region at different radii in the optimal flow. △, $r = 16{\cdot}1$ in.; □, $r = 17{\cdot}1$ in.; ○, $r = 17{\cdot}9$ in.

sequently, no information about the *instantaneous* shape or length of the turbulent region can be obtained from these measurements.

The effect of the length of the working space on the stability and intermittency of the optimal flow at $R_o = -50{,}000$, $R_i = 5600$ was briefly studied by moving both end plates inward to decrease L, keeping the probe fixed at $z = 0$, $r = 17$ in. The intermittency factor varied slowly with L, increasing from 0·58 at the maximum length of 54·7 in. to 0·62 at the minimum length of 34·0 in. However, there

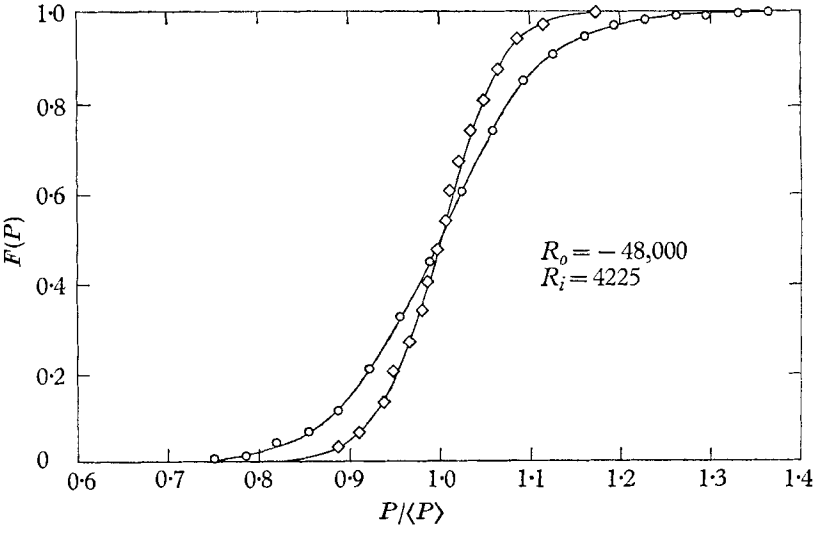

FIGURE 9. Distribution of interface position at different radii in a typical spiral turbulent flow. Data are for trailing interface (see figure 11). ○, $r = 16{\cdot}25$ in.; ◇, $r = 17{\cdot}00$ in.

was a striking change in the stability of the interface pattern as L decreased. The flow was very stable for L greater than 44 in., but became progressively more irregular as L was decreased below this value. For the minimum length, the hot-wire signals typically showed the usual alternation between laminar and turbulent flow for periods of several minutes, and then showed complete turbulence for intervals of 15–20 sec (5 to 7 periods of the normal intermittent signal). It was conjectured that decreasing the length of the apparatus increased the tendency for the flow to change hand spontaneously, and this conjecture was later verified by observations during which the hand of the flow was continuously monitored.

For fixed ω_o and ω_i, the angular velocity of the turbulence increased slightly as the length of the cylinders was decreased. This result is consistent with the previous observation that ω_i tends to follow the mean tangential velocity in the annulus, since the latter must increase with decreasing L due to the influence of the end plates rotating with the outer cylinder.

As a first step in investigating the two-dimensionality of the flow pattern in a helical co-ordinate system attached to the interfaces, the intermittency factor for $R_o = -50{,}000$, $R_i = 5600$ was measured as a function of axial position for two different radii. Since probes could be installed only at positions 1 ft. apart along the cylinders, measurements at intermediate stations were made by moving both end plates in the same direction, keeping the length of the working space fixed.

To allow this freedom, it was necessary to reduce the length of the working space to 46·7 in.

The interfaces were found to be sharply defined and stable for all axial locations. The measurements of γ, collected in figure 10, suggest a useful degree of two-dimensionality in the central region. On the other hand, there are regions at each end, accounting for 40–50 % of the (shortened) working space, in which significant axial variations may exist.

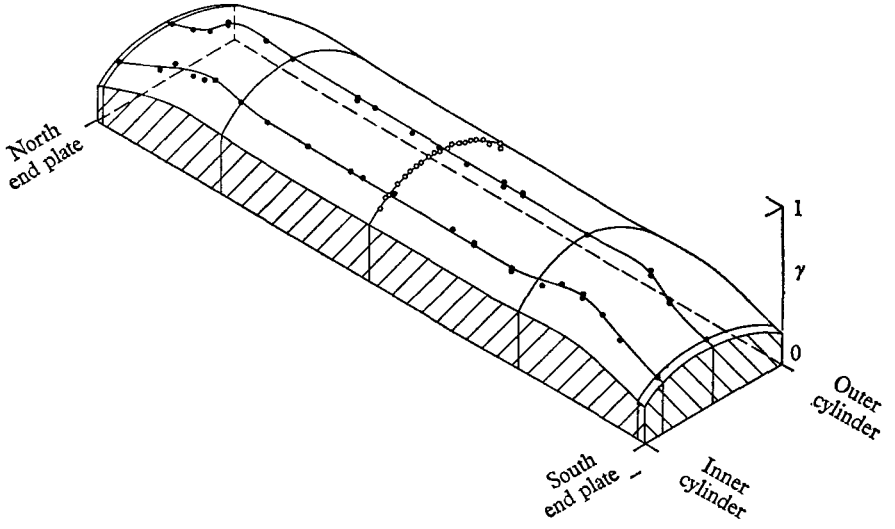

FIGURE 10. Axial variation of γ for $R_o = -50{,}000$, $R_i = 5600$. ○, $L = 54{\cdot}7$ in., $z = 0$; ●, $L = 46{\cdot}7$ in., $r = 16{\cdot}25$ in., 17·00 in.

Several methods have been used to measure the mean shape of the interface pattern in the optimal flow. All of these methods involved the use of two different hot wires. In the earliest measurements, the signals from two hot wires, mounted at different radial locations on a single probe, were added, and the interface pattern was inferred from the intermittency factors for the individual and combined signals. This method, unfortunately, was found to be inapplicable to a large fraction of the flow because of the geometrical character of the interface pattern. A different method was therefore adopted, using tape-recorded data,† to determine the average time interval between crossings of a given interface by two hot wires. One probe was kept fixed at $r = 17$ in., while the other (located 180° from the first) was traversed radially. Since the tapes could be played in either direction, the two interfaces could be observed independently.‡ The resulting interface-geometry data are shown in figure 11. The mean cross-section of the turbulent volume of fluid is roughly anti-symmetrical around

† The tape-recorded data in question are being used to determine mean and fluctuating velocity fields in the optimal spiral turbulence by means of digital sampling methods. A detailed discussion of the turbulence-discrimination and data-handling techniques had been given by Van Atta (1964).

‡ One residual problem in this method is that discrimination between laminar and turbulent flow is still being made in terms of fluctuating voltages rather than velocities. As part of the final data-processing operation, it is intended to re-measure the interface positions by digital discrimination on the sampled velocities.

$r = 17$ in., so that the interface pattern is nearly the same when observed from either of the two cylinders. A tail of turbulent fluid near $r = 16{\cdot}5$ in. is stretched out in the direction of motion of the inner cylinder, while a nose near $r = 17{\cdot}5$ in. is stretched out in the direction of motion of the outer cylinder. As a by-product of the measurement of mean interface position, the circumferential dispersion in this position was again measured, with the result shown in figure 12. Note that

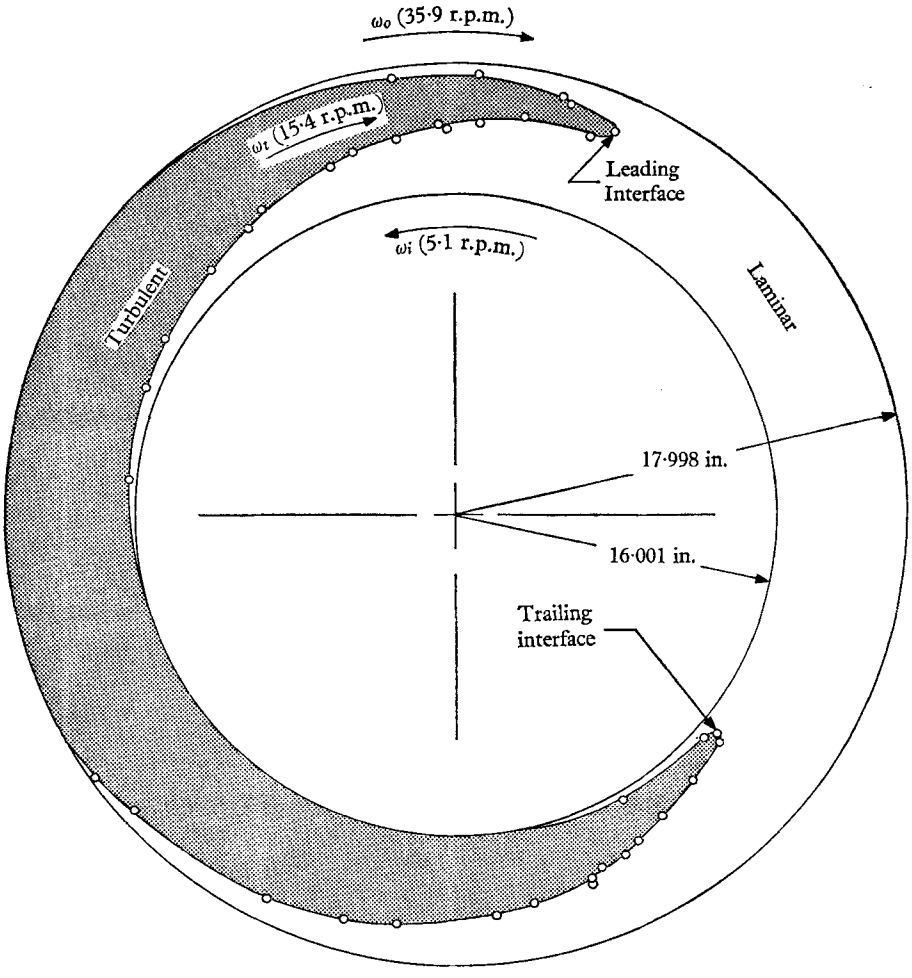

FIGURE 11. Mean interface geometry for the optimal flow (radial scale slightly expanded for clarity). Data based on approximately 3000 cycles of flow for each point on interface.

the dispersion in the leading interface (that is, leading in laboratory co-ordinates) is considerably smaller at all radii than the dispersion in the trailing interface.† This is the first evidence of any significant difference in the structure or behaviour of interfaces separating laminar and turbulent regions of the fluid.

† This terminology is not intended to be confusing. The 'leading' and 'trailing' interfaces extend from wall to wall and are labelled to correspond to the motion of the turbulent region in the inertial co-ordinate system of the laboratory. 'Transition' and 'anti-transition' interfaces, on the other hand, have been differently defined in § 1. Thus in figure 11 the outer half of the leading interface and the inner half of the trailing interface (i.e., the nose and tail referred to above) are anti-transition interfaces.

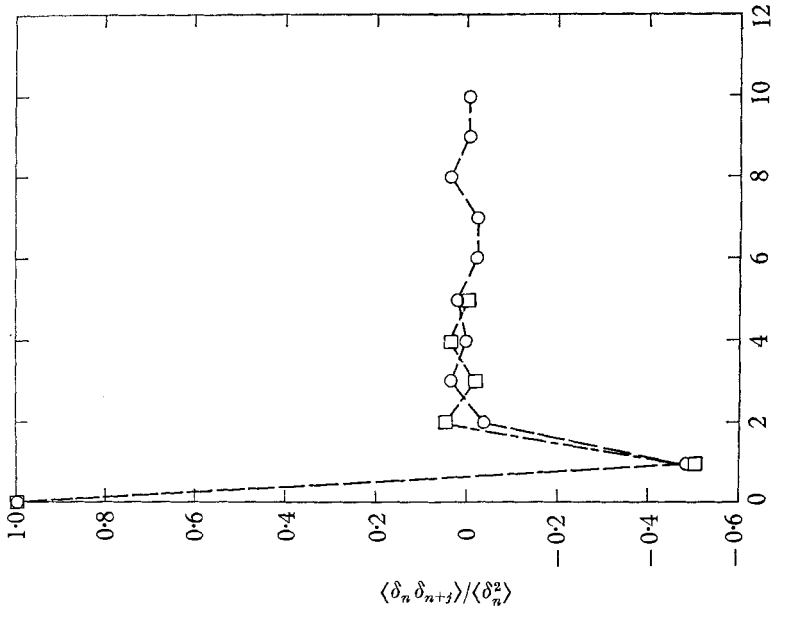

FIGURE 13. Example of serial correlation for interval between successive observations of one interface in the optimal flow. ○, Computer calculation: 3199 cycles of flow; $r = 16{\cdot}248$ in., $R_o = -50{,}000$, $R_i = 5600$. □, Manual calculation: 240 cycles of flow; $r = 16{\cdot}25$ in., $R_o = -49{,}000$, $R_i = 6350$.

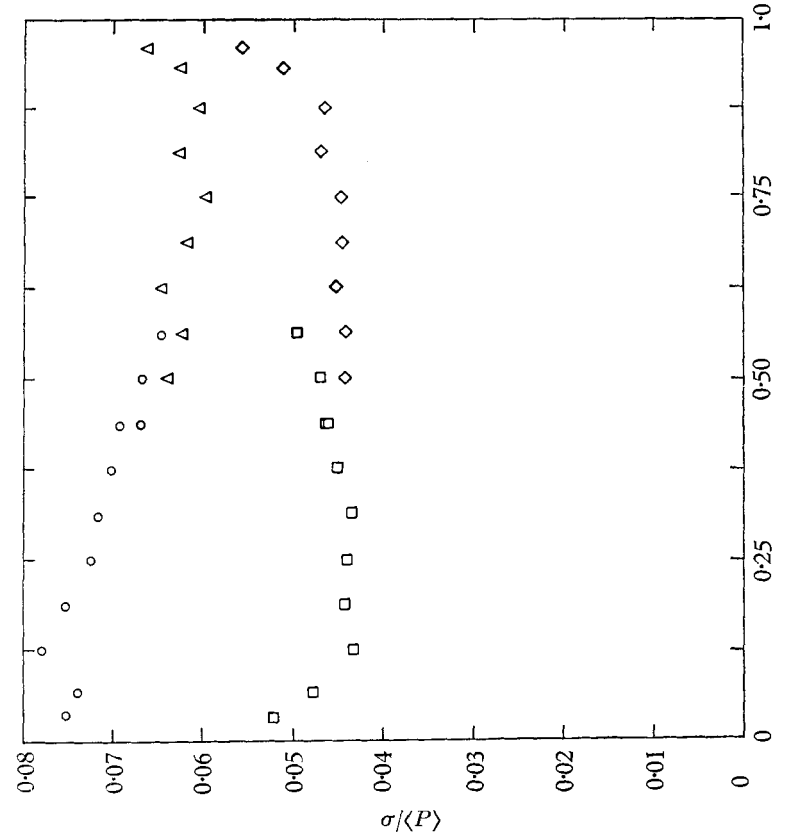

FIGURE 12. Standard deviation of interface location for leading and trailing interfaces. Leading interface: □, probe on outer cylinder; ◇, probe on inner cylinder. Trailing interface: ○, probe on outer cylinder; △, probe on inner cylinder.

8. Time scale for fluctuations in interface position

The present measurements give no information about the *instantaneous* shape or velocity of the interfaces. Measurement of instantaneous shape would require the employment of a large number of probes whose wakes might seriously modify the mean flow. Measurement of instantaneous velocity at a point on the interface presents a similar difficulty. The characteristic time scale for random fluctuations in interface position, however, was inferred indirectly during the study of mean

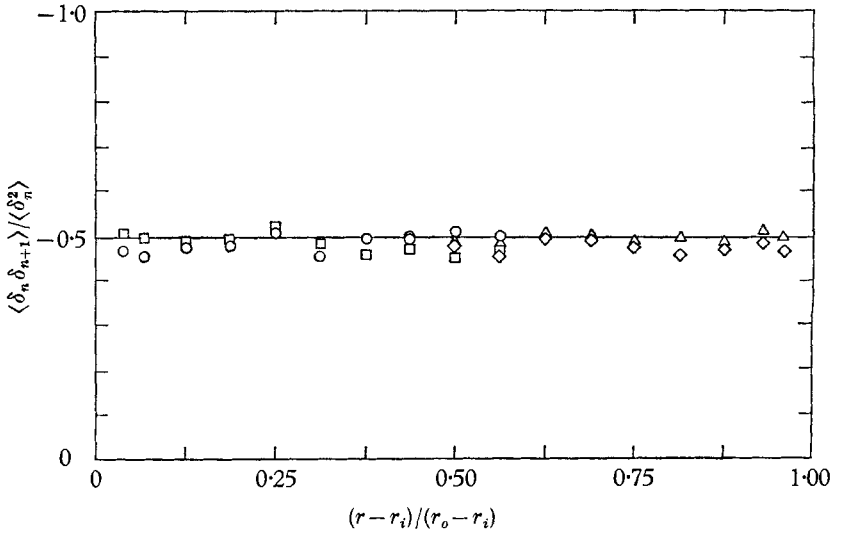

FIGURE 14. Correlation for adjacent intervals between successive observations of interface position in the optimal flow. Probe on outer cylinder: ○, trailing interface; □, leading interface. Probe on inner cylinder: △, trailing interface; ◇, leading interface.

interface position. Let $\delta_n = P_n - \langle P \rangle$ denote the deviation from the mean of a single time interval P_n, whose end points are determined by successive interface crossings. Let δ_{n+j} denote the corresponding deviation measured j intervals later. From the tape-recorded data, normalized correlations $\langle \delta_n \delta_{n+j} \rangle / \langle \delta_n^2 \rangle$ have been computed for values of j from 1 to 10 for various radii. As shown for one example in figure 13, the intervals are essentially independent† (more accurately, the correlation is essentially zero) for $j \geqslant 2$. The correlation between adjacent intervals ($j = 1$), shown in figure 14, lies consistently between $-0{\cdot}45$ and $-0{\cdot}52$ for all radial locations, showing that an interval longer than $\langle P \rangle$ is likely to be immediately followed by an interval shorter than $\langle P \rangle$. In fact, the observed correlations correspond closely to what would be expected if the characteristic time scale (correlation time) for random fluctuations in interface position were appreciably less than the time P_n required for the probe to traverse the flow pattern once. This assumption implies (see Appendix) that $\langle \delta_n \delta_{n+1} \rangle / \langle \delta_n^2 \rangle = -0{\cdot}5$ for $j = 1$ and

† This result was first obtained by hand computation for a single case, using a preliminary tape recording (at nearly the same radial location and Reynolds number) and the intermittency meter as described in § 6.

$\langle \delta_n \delta_{n+j} \rangle / \langle \delta_n^2 \rangle = 0$ for $j \geqslant 2$. The observed correlation of $-0{\cdot}45$ to $-0{\cdot}52$ for adjacent intervals, and the small values of the higher-order correlations, are therefore strong evidence that the interface memory or correlation time is appreciably less than P_n.

Appendix. Serial correlation for time interval between successive observations of a given interface

At a fixed radius, the angular position of a given interface in laboratory co-ordinates $\Theta(t)$ may be decomposed into mean and fluctuating parts. The mean part, $\omega_t t$, is a linear function of time, while the fluctuating part, $\theta(t)$, is a stationary stochastic function of time with zero mean. Suppose that the measuring probe is

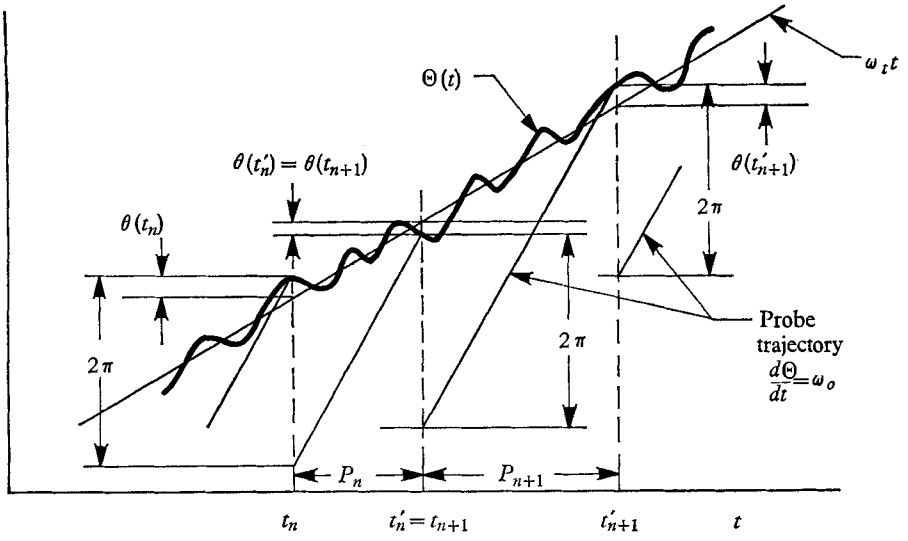

FIGURE A.1. Notation for equations of Appendix.

mounted on the outer cylinder (the argument is nearly identical for a probe on the inner cylinder). In the time interval, $P_n = t_n' - t_n$, between probe crossings of a given interface, the angular distance travelled by the probe is $\omega_o P_n$, while the angular distance travelled by the interface is $\omega_t P_n + \theta(t_n') - \theta(t_n)$. Allowing for the fact that the probe traverses the interface at the ends of the interval P_n (figure A.1), then

$$\omega_o P_{n+j} = 2\pi + \omega_t P_{n+j} + \theta(t_{n+j}') - \theta(t_{n+j}),$$

or, since

$$\theta(t_{n+j}) = \theta(t_{n+j-1}'),$$

$$\delta_{n+j} = P_{n+j} - \langle P \rangle = \frac{\theta(t_{n+j+1}) - \theta(t_{n+j})}{\omega_o - \omega_t}.$$

The normalized correlation between the fluctuation for one interval and the fluctuation for the jth following interval is therefore

$$\psi_j = \frac{\langle \delta_n \delta_{n+j} \rangle}{\langle \delta_n^2 \rangle} = \frac{2\langle \theta(t_n)\,\theta(t_{n+j}) \rangle - \langle \theta(t_n)\,\theta(t_{n+j-1}) \rangle - \langle \theta(t_n)\,\theta(t_{n+j+1}) \rangle}{2\langle \theta^2(t_n) \rangle - 2\langle \theta(t_n)\,\theta(t_{n+1}) \rangle}.$$

If the characteristic period of random fluctuations in interface position is negligibly small compared with P_n, then values of $\theta(t)$ separated by an interval equal to or greater than P_n will be uncorrelated; that is,

$$\langle \theta(t)\,\theta(t+T)\rangle = 0; \quad T \geqslant P_n.$$

If this is the case, then

$$\psi_j = \frac{\langle \delta_n\,\delta_{n+j}\rangle}{\langle \delta_n^2\rangle} = \begin{cases} 1 & j = 0, \\ -0{\cdot}5 & j = 1, \\ 0 & j \geqslant 2. \end{cases}$$

These results, which are independent of the distribution function for P, explain how a strong first-order ($j = 1$) correlation and negligible higher-order correlations can be obtained when a random variable is observed periodically and, compared with the correlation time for the fluctuations, relatively infrequently.

It has been implicitly assumed, in view of experimental evidence like that in figure 2, that fluctuations in interface position, although rapid, are slow enough for the probe to cross each interface only once (always in the same direction) during each encounter with the turbulent volume of fluid. For less regular cases, the interfaces may fluctuate so rapidly that they appear to be poorly defined, even though the interface itself remains sharp, and the argument given here might not apply.

This paper presents the results of one phase of research carried out at the Jet Propulsion Laboratory, California Institute of Technology, under Contract no. NAS 7-100, sponsored by the National Aeronautics and Space Administration.

REFERENCES

Coles, D. 1962 Interfaces and intermittency in turbulent shear flow. *Mécanique de la turbulence, CNRS*, Paris, pp. 229–48.

Coles, D. 1965 *J. Fluid Mech.* **21**, 385–425.

Coles, D. & Van Atta, C. 1966 *J. Fluid Mech.* **25**, 513.

Schultz-Grunow, F. 1959 *Z. angew. Math. Mech.* **39**, 101–10.

Van Atta, C. W. 1964 Ph.D. Thesis, California Institute of Technology.

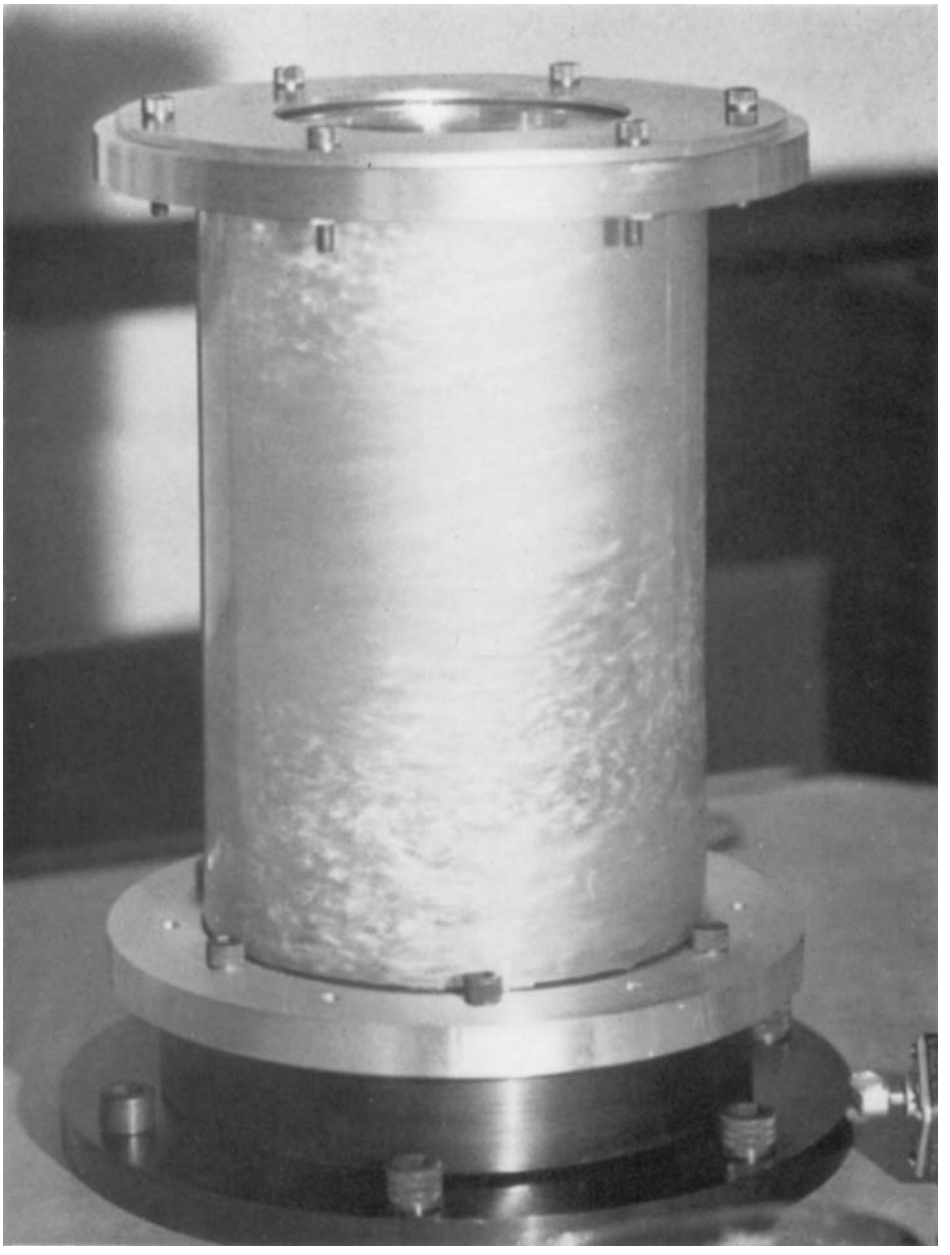

FIGURE 1. Spiral turbulence; flow visualization by Coles using suspension of aluminium powder in silicone oil. $R_o = -15{,}880$, $R_i = 5250$.

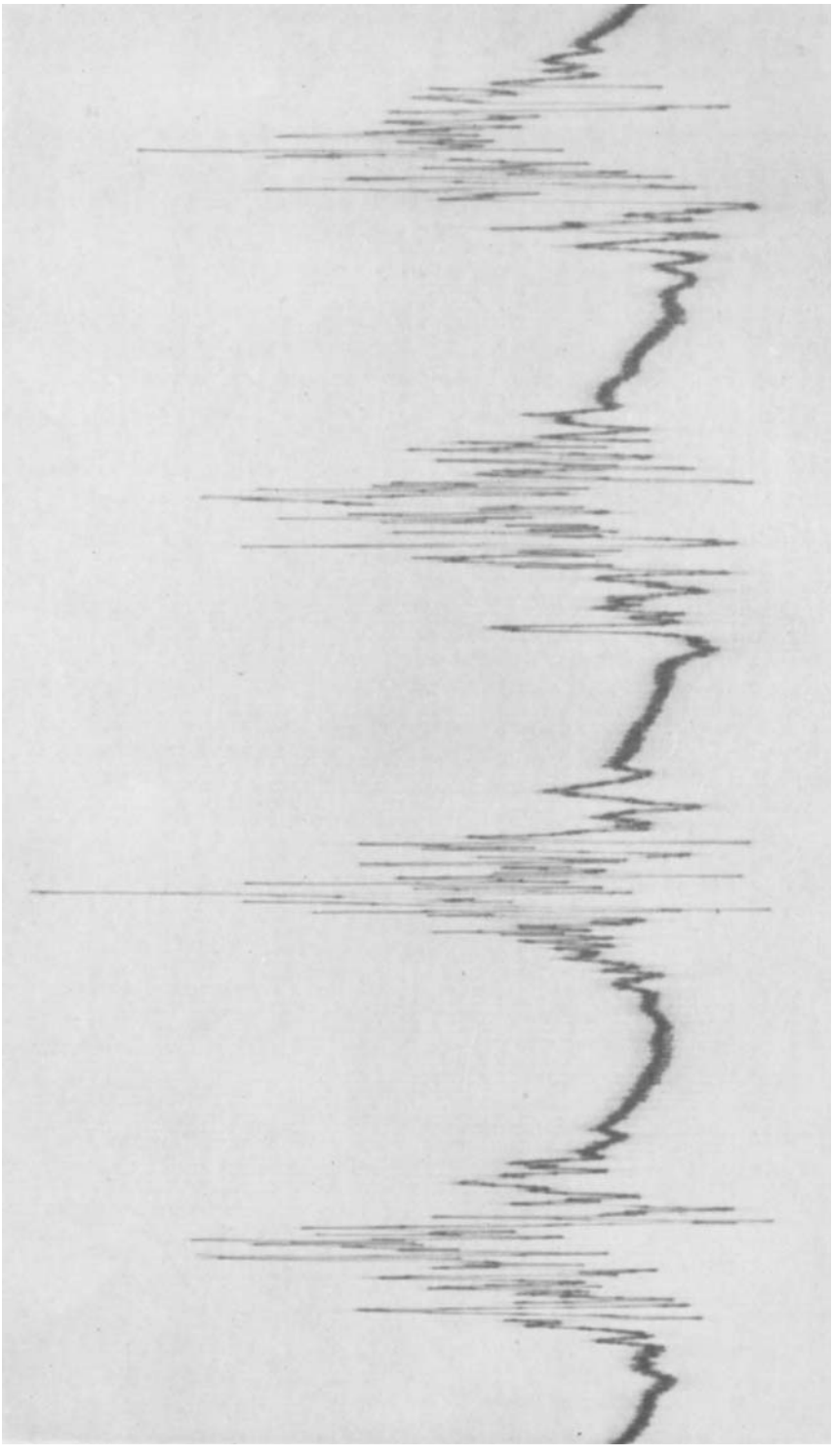

FIGURE 2. Typical hot-wire signal in spiral turbulence. $R_o = -50{,}000$, $R_i = 5600$. Probe mounted on outer cylinder at $r = 17{\cdot}125$ in.